

# 220,000-r/min, 2-kW Permanent Magnet Motor Drive for Turbocharger

Toshihiko Noguchi, Yosuke Takata \*

Yukio Yamashita, Yoshimi Komatsu, and Seiichi Ibaraki \*\*

This paper describes an ultra high-speed permanent-magnet synchronous motor drive, which is embedded in a turbocharger of an internal-combustion engine. The electric drive makes it possible to enhance output power of the turbocharger in a motoring mode and to retrieve combustion energy from exhaust gas in a regenerating mode. The rotor is composed of a mechanically reinforced high-performance Nd-Fe-B permanent magnet and its diameter is designed to be considerably small to prevent huge centrifugal force caused by the ultra high-speed rotation. The stator consists of a laminated iron-core with extremely thin (0.15 mm) electromagnetic steel plates to minimize the iron-core losses. Two types of the stator configurations, i.e., 3-slot and 6-slot stator designs are discussed from the viewpoint of magnetic field and losses analysis. Consequently, the latter design is found to be remarkably effective to suppress temperature rise of the rotor due to an eddy-current loss in the rotor permanent magnet. Also, it is indispensable to reduce the motor inductance less than 10 ( $\mu$ H) because dc bus voltage of an inverter is limited to 72 (V). A pseudo current-source inverter, which has a current controlled chopper across the dc bus, is employed to drive the motor with a 120-deg. conduction pattern because conventional sinusoidal PWM techniques are unable to regulate the motor current in such an ultra high-speed range. Computer simulations and experimental tests are conducted to examine various operation characteristics of a prototype. The experimental data demonstrate 220,000-r/min operation at 2.2-kW inverter output power, which agree with the simulation results well and prove feasibility of the proposed system.

**Keywords:** ultra high-speed PM motor, turbocharger, magnetic field analysis, losses analysis, pseudo current-source inverter

## 1. Introduction

Turbochargers are auxiliary machines of gasoline engines and diesel engines mounted on automobiles, vessels and so forth. Their principal objectives are improvement of combustion efficiency, output power and response of the engines over wide speed ranges. The turbochargers consist of a compressor, which compress vaporized fuel/air mixture, and a turbine, which rotates at an extremely high-speed with exhaust gas power. Since the compressor and the turbine are mechanically and directly coupled with a shaft, the conventional turbochargers have less controllability in terms of speed, torque and power flow. For example, it is difficult to avoid response delay, i.e., turbo lag, because compression of the vaporized fuel/air mixture does not begin without starting the turbine with the exhaust gas. In general, it is rather insufficient to overcharge the compressed fuel/air mixture into the engine cylinders at a low-speed range. Furthermore, although combustion energy is huge when the

engine rotates under high-speed and low-load conditions, it is hardly possible to retrieve combustion energy from the exhaust gas. All of these difficulties come from a pure mechanical structure of the conventional systems.

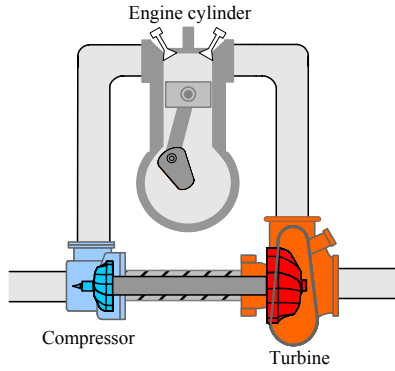
This paper proposes a novel hybrid system, which introduces power electronics, i.e., an ultra high-speed permanent-magnet synchronous motor (PMSM) drive, into the turbochargers, and describes computer simulation and experimental results of the adjustable speed drive followed by a motor design guideline on the basis of electromagnetic and losses analyses. The most difficult problem in this project is how to achieve an ultra high-speed operation such as 220,000 r/min at over 2-kW inverter output with the PMSM and how to raise power density of the motor embedded in the turbocharger. There are many other technical issues to surmount, e.g., bearings and mechanical shaft vibration, but this paper focuses on an electrical aspect of the motor and its adjustable speed drive.

## 2. Outline of Novel Hybrid Turbocharger

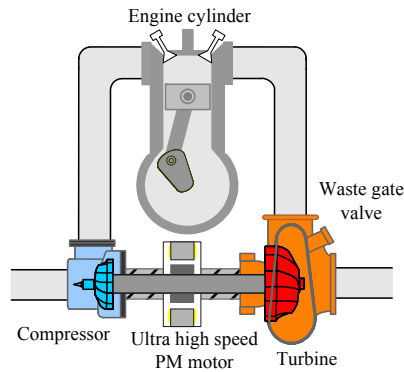
Fig. 1 (a) shows a conventional turbocharger. As described above, output pressure or a rotating speed of the compressor cannot easily be controlled because it mechanically depends on combustion energy of the exhaust gas from the engine. It is rather difficult to obtain sufficient compression of the fuel/air mixture at low-speed operation of the engine because the combustion energy of the exhaust gas retrieved by the turbine is relatively low. On the other hand, the exhaust gas is emitted to the open air

\* Nagaoka University of Technology, tnoguchi@vos.nagaokaut.ac.jp  
1603-1 Kamitomioka, Nagaoka 940-2188, JAPAN

\*\* Mitsubishi Heavy Industries, Ltd., yukio\_yamashita@mhi.co.jp  
Nagasaki Research & Development Center  
5-717-1 Fukahori, Nagasaki 851-0392, JAPAN  
This work has been supported by Grant-in-Aid for Scientific Research (B)(2) 16360137 from Ministry of Education, Culture, Sports, Science and Technology, Japan.



(a) Conventional turbocharger.



(b) Proposed hybrid turbocharger.

Fig. 1. Overviews of conventional and proposed turbochargers.

Table 1. Principal specifications of ultra high-speed PMSM drive.

Rated power (Cont.)	2 (kW)
Rated torque (Cont.)	0.159 (Nm)
Rated speed (Cont.)	120,000 (r/min)
Maximum speed	220,000 (r/min)
Overload	200 %-2 (s)

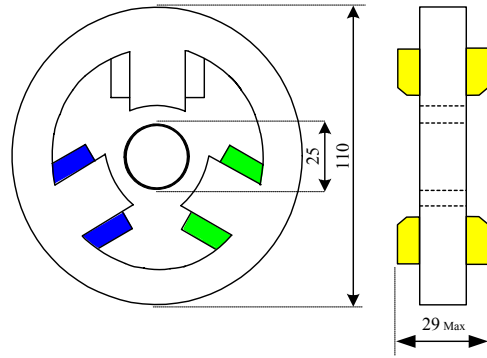
through a waste gate valve, and a large amount of the exhaust energy is disposed at high-speed and low-load operation of the engine. This occasion usually happens when the vehicle cruises at constant speeds on expressways.

The hybrid turbocharger proposed in this paper is depicted in Fig. 1 (b). An ultra high-speed PMSM is mounted between the compressor and the turbine on the shaft of the turbocharger, and is embedded in it. Motoring of the PMSM gives assisting torque to the compressor, which allows higher controllability of the compressed fuel/air mixture at any rotation of the engine. Also, the turbo lag is dramatically improved with the assisting torque of the motor. Furthermore, the exhaust energy can be retrieved by operating the PMSM as a generator, and can be stored in batteries as co-generated electric energy. This operation contributes improvement of the total efficiency from fuel to mechanical and electrical output power of the engine system.

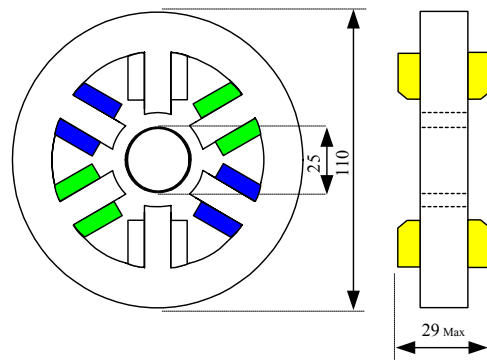
### 3. Ultra High-Speed PMSM

#### 3.1 Specifications of Ultra High-Speed PMSM

A technical target of the motor design is discussed in this section, which is needed in the above hybrid turbocharger. According to several matching simulation results of an



(a) 3-slot motor.



(b) 6-slot motor.

Fig. 2. Principal dimensions of 3-slot and 6-slot motors.

automobile engine and a turbocharger tested at Nagasaki Lab., Mitsubishi Heavy Industries, it has been inferred that the combustion efficiency and engine output can be improved by 8 % and 150 % by applying 1-kW assisting torque to the turbocharger, respectively. In addition, 12 % and 200 % improvement of them can be expected by giving 2-kW assisting torque to the turbocharger. From these estimation results, an ultra high-speed PMSM drive of which specifications are listed in Table 1 has been developed for the purpose of enhancement of combustion efficiency by 10 % and engine output by 200 %.

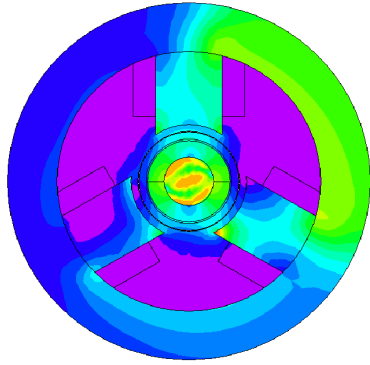
#### 3.2 Stator and Rotor Configuration

In order to optimize the motor configuration, two types of stators, i.e., a 3-slot stator and a 6-slot stator, along with one type of a rotor were investigated through electromagnetic analyses. Both types of the motors are two-pole machines to satisfy an extremely high-speed rotation and have concentrated stator windings to simplify the configuration and to reduce leakage inductance.

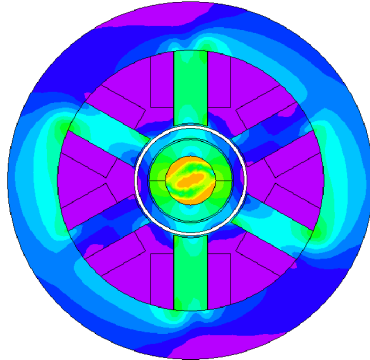
The number of turns per pole is expressed by the following equation;

$$N = \frac{E}{4.44k_d k_p \phi_m}, \dots\dots\dots (1)$$

where  $E$  is an induced voltage per pole,  $k_d$  is a distributed winding factor,  $k_p$  is a short pitch coefficient, and  $\phi_m$  is a total magnetic flux. Therefore, the distributed winding factors and the short pitch coefficients of the 3-slot machine and the 6-slot machine are derived as follows, respectively;



(a) Flux density of 3-slot motor.



(b) Flux density of 6-slot motor.

Fig. 3. Flux density distributions of 3-slot and 6-slot motors.

$$k_{d3} = k_{d6} = 1 ; \dots\dots\dots(2)$$

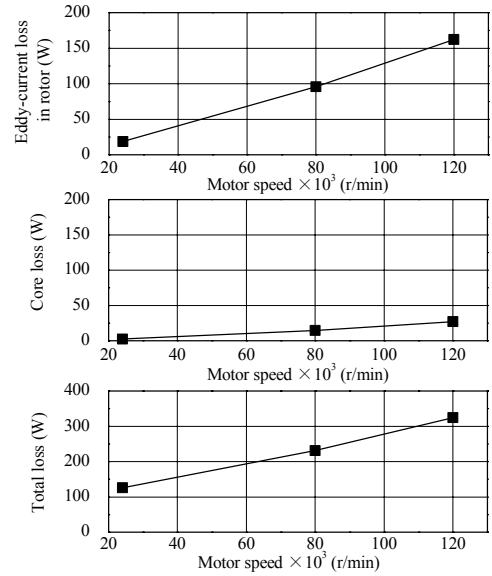
$$k_{p3} = \sin\left(\frac{2\pi}{3}\right) = 0.866 ; \dots\dots\dots(3)$$

$$k_{p6} = \sin\left(\frac{1\pi}{3}\right) = 0.5 . \dots\dots\dots(4)$$

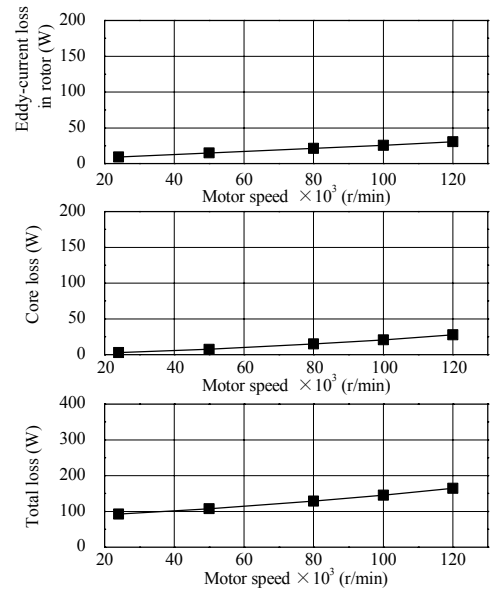
As shown in the above equations, the number of turns of the 3-slot machine is 0.58 times of that of the 6-slot one, which implies that the space factor of the former is superior to that of the latter. The PMSM to be designed in this paper can inherently be miniaturized because its fundamental operation frequency is approximately 3.67 (kHz), and further miniaturization is required to make the motor embedded in the turbocharger. In other words, it is indispensable to enlarge the power density of the machine from ordinary values of 0.8-1.4 (W/cm<sup>3</sup>) to 14 (W/cm<sup>3</sup>). Therefore, a great attention must be paid to losses of the motor as well as a cooling system design. Since the 3-slot machine has larger spatial harmonics than the 6-slot machine has, a large variation of the permeance possibly causes an eddy current loss in the rotor magnet. The eddy current loss results in considerable temperature rise and fatal demagnetization of the permanent magnet.

**3.3 Electromagnetic Analyses Result**

Losses analyses of the 3-slot motor and the 6-slot motor were conducted with a boundary element method and a finite element method. Fig. 2 (a) and (b) show principal dimensions of both motors. The outer diameters of the stator and the rotor are 110 (mm) and 25 (mm), respectively. The motors have a wide air gap of 5 (mm), which is almost



(a) Losses of 3-slot motor.

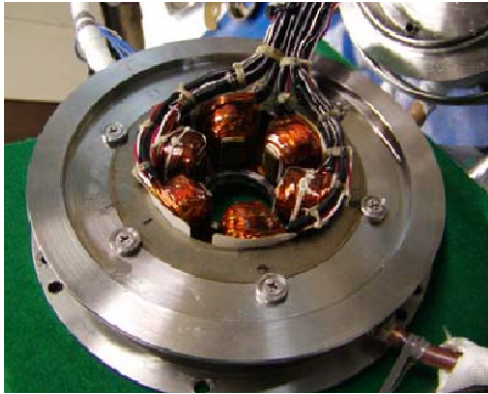


(b) Losses of 6-slot motor.

Fig. 4. Losses analysis results of 3-slot and 6-slot motors.

same as thickness of the permanent magnet on the rotor. A Nd-Fe-B high-performance permanent magnet of 39-MGOe maximum energy product is employed on the rotor, and 0.15-mm thick electromagnetic silicon steel plates are used to compose the laminated stator core.

Fig. 3 and Fig. 4 show electromagnetic analysis results and losses analysis results at 2-kW output power, respectively. It can be seen that the 3-slot motor generates higher eddy current loss in the rotor permanent magnet, which is approximately five times of that of the 6-slot motor. This eddy current is caused by the spatial harmonics associated with the flux variation as described above. However, there are not significant differences between the two motors in terms of a copper loss and an iron loss of the stator. Consequently, it can be found that the 6-slot motor has great advantage over the 3-slot motor in reducing the resultant total losses, which is



(a) 6-slot stator of prototype.



(b) Rotor of prototype.

Fig. 5. Photographs of prototype machine.

approximately 50 % of the 3-slot motor's losses.

### 3.4 Implementation of Prototype Machine

Fig. 5 shows photographs of a prototype machine, where the 6-slot stator with the concentrated windings and the mechanically reinforced permanent-magnet rotor can be seen. As is described in the computer analyses, the concentrated stator windings are employed to reduce winding resistance and leakage inductance, of which wires are 3.5-mm<sup>2</sup> PEW. The stator is composed of a laminated core of which each steel plate thickness is 0.15 (mm). In general, the most important design parameters of ultra high-speed machines are the stator inductance and resistance, and they are only 9 (μH) and 5.2 (mΩ) in this prototype, respectively. On the other hand, a Nd-Fe-B permanent magnet of which maximum energy product is from 39 to 43 (MGOe) is mounted on the rotor with an adhesive, and is magnetized to hold a sinusoidal MMF distribution. The rotor is physically reinforced by carbon fiber and some chemicals to prevent the permanent magnet from scattering by huge centrifugal force. The air gap is as wide as 5 (mm), but is good enough to hold appropriate flux density level. Fig. 6 illustrates a rotating part and bearings configuration of the hybrid turbocharger. Highly stable slip bearings are employed to support the shaft, and are located between the turbine and the rotor. This overhung structure is effective to simplify the whole assembly of the turbocharger.

### 4. Pseudo Current-Source Inverter

In general, a voltage-source PWM inverter with current minor loops is often used to drive a PMSM. Also, vector

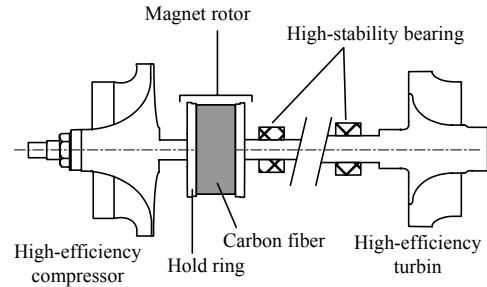


Fig. 6. Axial configuration of hybrid turbocharger.

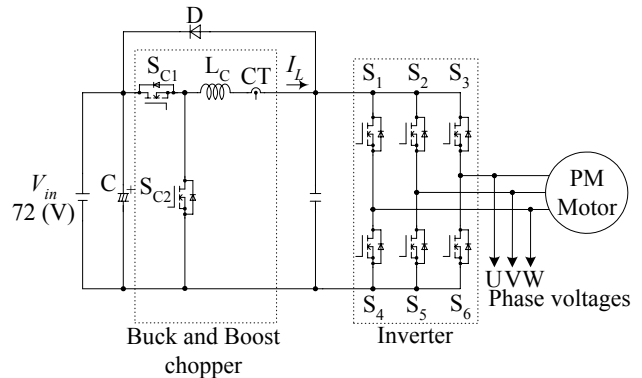
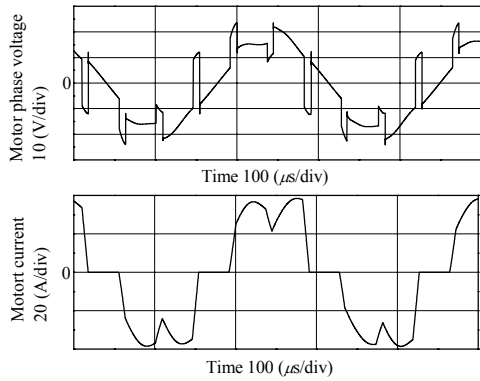


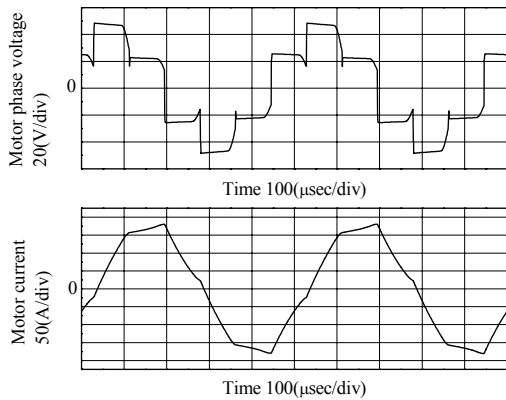
Fig. 7. Schematic diagram of pseudo current-source inverter.

control is adopted in the microcomputer-based system, which requires coordinate transforms and sinusoidal current regulation. However, since the fundamental frequency of the motor reaches as high as 3.67 (kHz) at the maximum operating speed, it is hardly possible to regulate the motor currents with an IGBT or FET based PWM inverter. Thus a pseudo current-source inverter shown in Fig. 7, which has a current controlled chopper across the dc bus, is employed to drive the motor with a 120-deg. conduction pattern because conventional sinusoidal PWM techniques are not suitable to regulate the motor current in such an ultra high-speed range. The motor current amplitude is controlled with a pulse amplitude modulation (PAM) technique by controlling the chopper duty ratio. Since a switching frequency of the chopper is as high as 30 (kHz), it is possible to reduce inductance of the dc bus reactor and to improve response of the dc bus current. At every moment of commutation in the 120-deg conduction inverter, surge voltages are caused by the winding inductance of the motor. These surge voltages are clamped by the dc bus voltage through a bypass diode of the chopper and body diodes in the FETs of the inverter. Therefore, it is not necessary to implement blocking diodes series with the FETs like most conventional current-source inverters require. In regenerating mode of the motor, kinematic energy is retrieved to the dc bus by operating the inverter as a 120-deg conduction synchronous switched mode rectifier.

Commutation of the inverter is carried out on the basis of an e.m.f. based mechanical sensorless control algorithm of the PMSM. The 120-deg conduction pattern is simply generated from the detected terminal voltages by using integrators to calculate the flux linkage and several logic ICs. Indeed, an initial flux position cannot be detected with this algorithm because there is no e.m.f. at the initial



(a) Phase voltage and current waveforms at 220,000 (r/min) and 2.2-kW inverter output.



(b) Phase voltage and current waveforms at 120,000 (r/min) and 200% overload.

Fig. 8. Operating waveforms (simulation results).

stand-still state; hence, open loop control is adopted to start up the motor until the operating speed reaches 10,000 (r/min). After reaching this speed threshold, the 120-deg conduction pattern is switched over to that generated from the e.m.f. based algorithm.

### 5. Operation Characteristics Examined through Computer Simulation

Prior to experimental tests, several computer simulations were conducted to confirm the basic operation characteristics of the proposed system. The test motor has identical specification as listed in Table 1, and the pseudo current-source inverter has 72-V dc bus voltage and 0.15-mH reactor in the chopper.

Fig. 8 (a) shows a simulation result of operation at the maximum speed of 220,000 (r/min) and 2.2-kW inverter output. As can be seen in this figure, the pulse voltage waveforms are observed at every instance of the commutation, and are clamped by the dc bus voltage. Since the rising and falling rates of the current during the commutation are restricted by the clamp voltage, reducing the total inductance of the motor is significantly important. Otherwise it is impossible to raise the fundamental operation frequency up to a few kHz with a proper 120-deg conduction pattern. Moreover, high fundamental displacement power factor operation is confirmed because the motor current is in phase with the phase voltage.

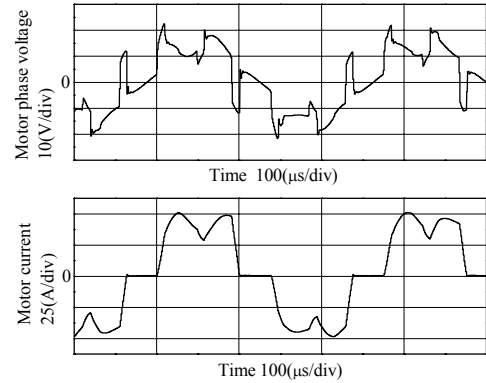


Fig. 9. Phase voltage and current waveforms at 220,000 (r/min) and 2.2-kW inverter output (experimental result).

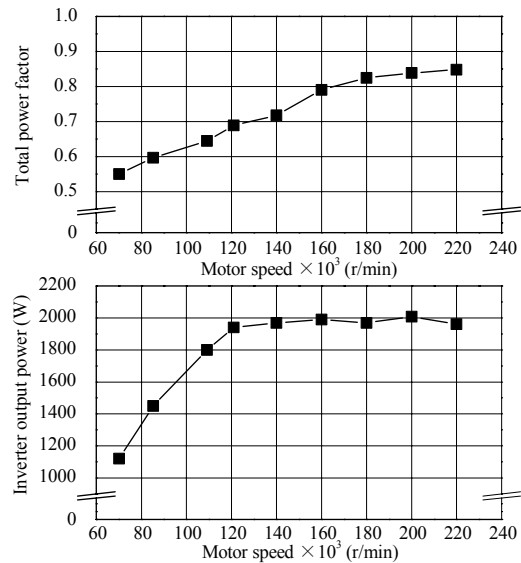


Fig. 10. Total power factor and inverter output.

Fig. 8 (b) depicts another simulation result at 200% overload condition at 120,000 (r/min). As described above, the commutation takes a longer time as the current amplitude is enlarged with the load because the clamp voltage limits the rising and falling rates of the current during the commutation. The situation shown in this figure is a limitation of the pseudo current-source inverter, and it is apparently impossible to enlarge the current amplitude higher than this condition, i.e., 200% load.

### 6. Experimental Setup and Results

Several experimental tests were conducted using a test hybrid turbocharger and a test pseudo current-source inverter. The first test was carried out to examine motoring operation, where the turbine was rotated by an external air flow source and giving assisting torque with the ultra high-speed PMSM to the compressor. During all time in this test, temperature of the stator windings was carefully watched, using thermo couplers.

Fig. 9 shows an experimental result at the maximum speed of 220,000 (r/min) and 2.2-kW inverter output. As can be measured in this test, the motor current is almost in phase with the phase voltage, and the both waveforms agree well with those of the simulation result. The total power

factor was 0.84 because both of the voltage and the current include a large amount of harmonics, while the excellent fundamental displacement power factor can be confirmed in the figure. The temperature of the stator windings rose to 120°C at continuous operation of the 120,000-r/min rated speed and the 2.2-kW inverter output. Therefore, it is indispensable to lower the temperature to prevent demagnetization of the rotor and hazardous overheat in the future work, not only improving the whole configuration of the turbocharger but also refining the motor design. In addition, it was confirmed that the 1.3-kW regenerative power was obtained at the rated speed.

Fig. 10 shows the total power factor and the inverter output power with respect to the motor speed. As can be seen in this figure, the total power factor did not exceed 0.84 because of the current waveform distortion caused by the 120-deg conduction waveforms. However, a constant torque operation and a constant power operation were satisfactory achieved below and over the rated speed of 120,000 (r/min), respectively.

## 7. Conclusion

This paper focused on a hybrid system that consists of the ultra high-speed PMSM embedded in the turbocharger, and described the motor design and adjustable speed drive characteristics of the hybrid system through experimental tests as well as computer simulations. According to the electromagnetic analyses of a 3-slot machine and a 6-slot machine, the former has disadvantage in terms of an eddy current loss in the rotor magnet, which is caused by the spatial harmonics of the 3-slot stator, but superior to the latter from the viewpoint of the space factor and heat emission of the stator. To the contrary, the 6-slot motor is able to reduce the eddy current loss of the rotor, which results in nearly 50-% total loss reduction.

A prototype system of the hybrid turbocharger, which consists of a two-pole and 6-slot PMSM and a pseudo current-source inverter, was developed on the basis of the above electromagnetic and losses analyses. Computer simulation results and experimental results agreed very well, and it was confirmed that continuous operation was achieved at 2.2-kW inverter output and at 120,000-r/min rated speed as well as at 220,000-r/min maximum speed.

## Acknowledgment

The authors wish to express their sincere thanks to colleagues and technicians who supported testing of the experimental setup at Nagasaki Lab., Mitsubishi Heavy Industries.

## References

- (1) Koichi Shigematsu, Jun Oyama, Tsyoshi Higuchi, Takashi Abe, and Yasuhiro Ueno, "The Novel Approach of Coupled Analysis for Small Size and Ultra-High Speed Motor," *IEE-Japan Proc. IAS Annual Conference*, no.85, p. 349, 2003 (in Japanese).
- (2) Mitsukichi Okawa, "Design Manual of Magnetic Circuit and PM Motor," Sogo Research, 1989 (in Japanese).
- (3) Takehisa Koganezawa, Isao Takahashi, and Kazunobu Oyama, "Sensorless Speed Control of a PM Motor by a Quasi-Current Source Inverter," *IEE-Japan Proc. IAS Annual Conference*, no. 45, p. 175, 1992 (in Japanese).
- (4) Yosuke Takata, Toshihiko Noguchi, Yukio Yamashita, Yoshimi Komatsu, and Seiichi Ibaraki, "220000r/min, 2-kW PM Motor Drive for Turbocharger", *IEE-Japan Proc. IAS Annual Conference*, no. 9, p. 155, 2004 (in Japanese).
- (5) Bon-Ho Bae, and Seung-Ki Sul, "A Compensation Method for Time Delay of Full-Digital Synchronous Frame Current Regulator of PWM AC Drives," *IEEE Trans. on Industry Applications*, vol. 39, no. 3, p.p. 802-810, 2003.
- (6) Bon-Ho Bae, Seung-Ki Sul, Jeong-Hyeck Kwon, and Ji-Seob Byeon, "Implementation of Sensorless Vector Control for Super-High-Speed PMSM of Turbo-Compressor," *IEEE Trans. on Industry Applications*, vol. 39, no. 3, p.p. 811-818, 2003.